Biointerface Research in Applied Chemistry
Open-Access Journal (ISSN: 2069-5837)

Article
Volume 16, Issue 2, 2026, 66
https://doi.org/10.33263/BRIAC162.066

Computational Screening of Benzimidazole Derivatives as Potential Anti-Alzheimer's Agents: An *In silico* Approach

Gigi G P [1], Uttam A. More [2], Prema Suseela [3,*]

[1] Department of Pharmaceutical Chemistry, College of Pharmacy, Shaqra University, Al Dawadimi, Kingdom of Saudi Arabia; gigisam@su.edu.sa;
[2] Department of Pharmaceutical Chemistry, Shree Dhanvantary Pharmacy College, Kim, 394110, Gujarat, India; uttamsrkv@gmail.com;
[3] Department of Pharmaceutical Chemistry, Crescent School of Pharmacy, B.S. Abdur Rahman Crescent Institute of Science and Technology, Vandalur, Chennai, India; prema.pharm@crescent.education;
* Correspondence: prema.pharm@crescent.education;

Received: 6.04.2025; Accepted: 21.07.2025; Published: 15.04.2026

Abstract: Alzheimer's disease (AD) is a progressive neurodegenerative disorder characterized by memory loss and cognitive decline. Targeting key enzymes such as acetylcholinesterase (AChE) and beta-secretase 1 (BACE-1) has emerged as a promising therapeutic strategy. This study utilized a structure-based virtual screening approach to identify dual inhibitors from a library of 431 benzimidazole derivatives retrieved from the ZINC database. Using the Schrödinger software suite, the compounds were evaluated using a multi-stage docking protocol that included QikProp ADME prediction, Lipinski's rule filtration, ligand preparation, and hierarchical molecular docking (HTVS, SP, and XP modes). Four top-ranking compounds were identified, with ZINC000558477778 and ZINC000614968635 exhibiting the highest binding affinities against AChE (-19.087 kcal/mol) and BACE-1 (-7.43 kcal/mol), respectively. Two other molecules, ZINC000558477776 and ZINC000558477775, showed strong dual-binding potential. These hits demonstrated favorable ADME profiles, CNS penetration, high oral absorption, and compliance with drug-likeness criteria. Toxicity analysis revealed non-mutagenicity and moderate acute toxicity. Overall, this study highlights benzimidazole derivatives as promising dual-target leads for further development as anti-Alzheimer's agents.

Keywords: benzimidazole derivatives; virtual screening; AChE and BACE-1 inhibitors; molecular docking; anti-Alzheimer agents.

1. Introduction

Alzheimer's disease (AD) is a chronic neurodegenerative disorder first described by Alois Alzheimer in 1906. It is the most prevalent form of dementia and represents a major global health challenge, with approximately 50 million people affected worldwide as of 2015. The projected increase to 131.5 million cases by 2050 poses significant social and financial burdens. AD is primarily characterized by progressive memory loss, cognitive decline, and behavioral impairments that worsen over time. These symptoms are largely associated with the degeneration of cholinergic neurons and the accumulation of amyloid-beta (Aβ) plaques and neurofibrillary tangles (NFTs) in the brain [1,2].

The key pathological features of Alzheimer's disease (AD) are the accumulation of amyloid-β (Aβ) plaques in the extracellular space and the formation of intracellular neurofibrillary tangles (NFTs) composed of abnormally hyperphosphorylated tau protein. The Aβ peptides, predominantly $A\beta_{40}$ and $A\beta_{42}$, are produced through the sequential proteolytic processing of amyloid precursor protein (APP) by β-secretase (BACE-1) followed by γ-secretase. Inefficient clearance of these peptides contributes to synaptic impairment, neurotoxic effects, and progressive neuronal loss [3–5]. Under normal conditions, tau protein plays a crucial role in stabilizing microtubules; however, in AD, it undergoes abnormal hyperphosphorylation, particularly at residues T231, S396, and S422. This modification reduces its affinity for microtubules, destabilizing them. Consequently, tau aggregates into insoluble paired helical filaments that form neurofibrillary tangles (NFTs), ultimately impairing axonal transport and disrupting neuronal function. These pathological changes impair neuronal transport mechanisms, further exacerbating neurodegeneration [6–8]. Recent evidence (2023) has further highlighted the strong association between tau hyperphosphorylation and neuroinflammatory responses, suggesting that inflammatory mechanisms play a significant role in promoting tau aggregation and accelerating disease progression [9].

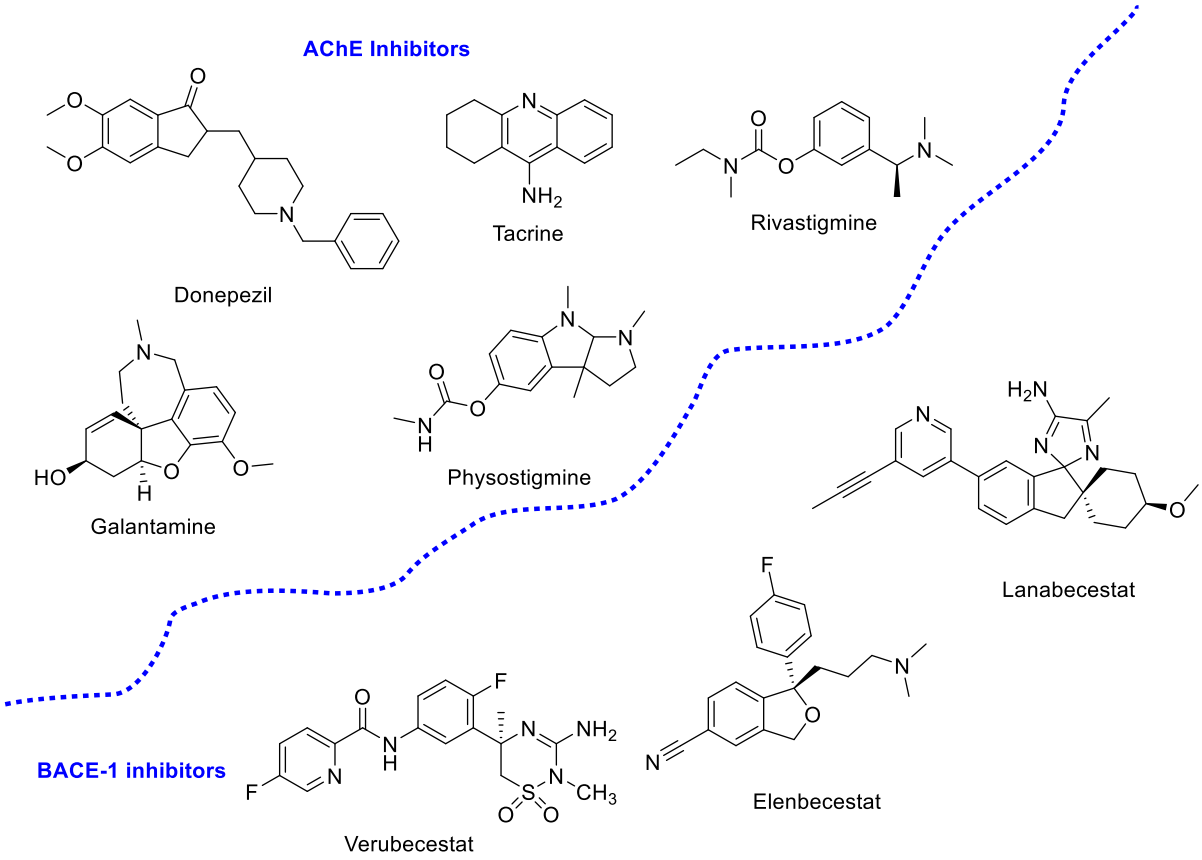

Figure 1. Well-known inhibitors of AChE and BACE-1.

BACE-1 is a key enzyme in the amyloidogenic processing of APP, initiating the formation of Aβ peptides. Increased expression and enzymatic activity of BACE-1 have been observed in both the brain tissue and cerebrospinal fluid of individuals with AD, further supporting its significance as a crucial therapeutic target [10–12]. Despite extensive efforts, clinical trials for BACE-1 inhibitors (Figure 1), such as Verubecestat and Lanabecestat, have largely failed due to adverse effects and lack of efficacy in later stages of AD. These failures highlight the complexities of targeting BACE-1 while maintaining normal physiological

functions [13,14]. Recent 2024 reviews emphasize that extensive inhibition of BACE-1 activity, typically exceeding 50%, can interfere with essential physiological processes in the brain, leading to adverse effects such as cognitive decline and synaptic dysfunction. In contrast, a more moderate and selective inhibition of around 30% is suggested to achieve a better therapeutic balance, sufficiently reducing amyloid-β production while minimizing off-target effects and preserving normal BACE-1 functions necessary for neuronal health [15]. Current research efforts are increasingly focused on developing highly selective BACE-1 inhibitors, along with multitarget therapeutic strategies that simultaneously address both amyloid and tau pathologies. These approaches aim to effectively reduce pathological processes while preserving BACE-1's normal physiological functionso minimize adverse effects [16].

Acetylcholinesterase (AChE), another key enzyme implicated in AD, hydrolyzes acetylcholine (ACh), a neurotransmitter essential for learning and memory. The cholinergic hypothesis of AD postulates that a loss of cholinergic neurons leads to cognitive decline. AChE inhibitors (Figure 1), such as donepezil, rivastigmine, and galantamine, have been approved to alleviate symptoms by enhancing cholinergic transmission [17–19]. However, these drugs do not halt disease progression, necessitating the exploration of novel multi-targeted therapies.

Given the multifactorial nature of AD, a single-drug, single-target approach has proven insufficient. The multi-target directed ligand (MTDL) strategy aims to develop compounds that simultaneously inhibit multiple pathological pathways. Gong *et al*. proposed a multi-target drug therapy strategy (MTDTs), which offered a novel perspective for drug discovery. As a result, the creation of synergistic multi-target inhibitors has emerged as a more promising approach for treating diseases, particularly those arising from complex etiologies like Alzheimer's disease (AD). Acetylcholinesterase (AChE) is often considered a primary target, and it can be combined with other relevant targets in the design and synthesis of multi-target-directed ligands (MTDLs). Examples of such combinations include AChE and glycogen synthase kinase-3 beta (GSK-3β), AChE and beta-site amyloid precursor protein cleaving enzyme 1 (BACE-1), AChE and monoamine oxidase (MAO), as well as AChE and phosphodiesterase (PDE). Dual inhibition of BACE-1 and AChE is particularly promising, as it addresses both amyloidogenesis and cholinergic dysfunction [20,21]. Benzimidazole derivatives have emerged as potential candidates for this approach due to their diverse biological activities [22–24], including anti-inflammatory [25,26], antioxidant [27–29], and neuroprotective effects [30–32].

In the present study, 431 benzimidazole derivatives were retrieved from the ZINC database and subjected to molecular docking studies using Schrödinger software to assess their potential as dual inhibitors of BACE-1 and AChE. Molecular docking techniques enable the identification of promising drug candidates by predicting their binding affinity and interaction with target proteins. This *in silico* approach significantly reduces the time and cost associated with traditional drug discovery methods [33,34].

Benzimidazole scaffolds have demonstrated promising biological activity across multiple therapeutic areas, including anti-inflammatory, antioxidant, and neuroprotective activities. The presence of heteroaromatic nitrogen atoms within these molecules enables strong interactions with biological targets, including AChE and BACE-1 [35–37]. Given the structural diversity and high binding affinity of benzimidazole derivatives, computational screening can effectively identify potential lead compounds that may serve as anti-Alzheimer’s agents. Alzheimer's disease remains an urgent medical challenge with no curative treatment available. Dual-target inhibitors that simultaneously modulate AChE and BACE-1 offer a

novel therapeutic avenue [38,39]. This study explores the potential of benzimidazole derivatives as promising candidates for AD treatment through computational screening and molecular docking analyses. In this study, an *in silico* approach was employed to screen a library of benzimidazole-based molecules for their inhibitory potential against AChE and BACE-1 using molecular docking strategies. Simultaneous inhibition of AChE and BACE-1 presents a promising dual-action therapeutic approach for Alzheimer's disease, aiming to provide symptomatic improvement through AChE inhibition while slowing disease progression by reducing Aβ production via BACE-1 inhibition. Incorporating both targets in molecular docking studies represents a rational strategy for the discovery and design of multi-target-directed ligands (MTDLs) with potential efficacy in AD treatment.

2. Materials and Methods

All the computational studies, like ADMET, Virtual screening, and Molecular Docking, were carried out by Maestro (Schrodinger Inc.).

2.1. Data collection and ligand preparation.

A set of 431 benzimidazole derivatives was obtained from the ZINC database [40] (Supplementary file Table S1). All compounds were prepared using LigPrep [41], which generates multiple structures from each input structure with different ionization states, tautomers, stereochemistry, and ring conformations. This process helps eliminate unsuitable molecules based on criteria such as molecular weight or specified functional groups. Optimization was performed using the OPLS-2005 force field to obtain the low-energy conformer of each ligand. Table 1 represents the 42 molecules selected for the AChE target and the 41 molecules selected for the BACE-1 target after SP-docking.

Table 1. Chemical Structures (SMILES) and Identifiers of the Compounds Used in the Screening Library

Compound ID	Smiles
AChE Target	
ZINC000065927782	CCn1c([C@H](C)NC(=O)C2CCN(Cc3ccccc3)CC2)nc2ccccc21
ZINC000065928342	CCn1c(CCNC(=O)C2CCN(Cc3ccccc3)CC2)nc2ccccc21
ZINC000066989628	Cn1c(CNCC2CCN(Cc3ccccc3)CC2)nc2ccccc21
ZINC000157781533	Cn1c(CNC(=O)C2(C)CCN(Cc3ccccc3)CC2)nc2ccccc21
ZINC000180051082	C[C@@H](NCC1CCN(Cc2ccccc2)CC1)c1nc2ccccc2n1C
ZINC000184772972	CN(Cc1nc2ccccc2n1C)C(=O)C1(C)CCN(Cc2ccccc2)CC1
ZINC000184798904	C[C@@H](NC(=O)C1(C)CCN(Cc2ccccc2)CC1)c1nc2ccccc2n1C
ZINC000237857548	Cn1c(CNCC2CCN(Cc3ccccc3Cl)CC2)nc2ccccc21
ZINC000264727521	Cn1c(CCNC(=O)C2CCN(Cc3ccccc3)CC2)nc2cc(F)ccc21
ZINC000268676652	Cc1cccc2nc(CNC(=O)C3CCN(Cc4ccccc4)CC3)n(C)c12
ZINC000433128238	Cn1c(CCN2CCC3(CCN(Cc4ccccc4)CC3)C2)nc2ccccc21
ZINC000483048193	CC1(C(=O)NCCc2nc3ccccc3n2C(F)F)CCN(Cc2ccccc2)CC1
ZINC000511403859	O=C(NCCc1nc2ccccc2n1C(F)F)C1CCN(Cc2ccccc2)CC1
ZINC000511472161	CC(C)n1c([C@H]2CCCN(C(=O)C3CCN(Cc4ccccc4)CC3)C2)nc2ccccc21
ZINC000541572808	Cn1c(CCNC(=O)C2(C)CCN(Cc3ccccc3)CC2)nc2ccc(F)cc21
ZINC000543433796	Cn1c(CCNC(=O)C2(C)CCN(Cc3ccccc3)CC2)nc2cc(F)ccc21
ZINC000544388998	CCn1c(CCNC(=O)C2(C)CCN(Cc3ccccc3)CC2)nc2ccccc21
ZINC000544391540	CC(C)n1c(CCNC(=O)C2(C)CCN(Cc3ccccc3)CC2)nc2ccccc21
ZINC000554959923	O=[N+]([O-])c1ccc2nc(CN3C[C@H]4CCN(Cc5ccccc5)C[C@H]4C3)[nH]c2c1
ZINC000554963001	CCn1c(CN2C[C@H]3CCN(Cc4ccccc4)C[C@H]3C2)nc2cc(F)ccc21
ZINC000554963003	CCn1c(CN2C[C@H]3CCN(Cc4ccccc4)C[C@@H]3C2)nc2cc(F)ccc21
ZINC000558477775	Cn1c(CCN2C[C@H]3CN(Cc4ccccc4)CC[C@H]3C2)nc2ccccc21
ZINC000558477776	Cn1c(CCN2C[C@H]3CCN(Cc4ccccc4)C[C@@H]3C2)nc2ccccc21
ZINC000558477777	Cn1c(CCN2C[C@H]3CCN(Cc4ccccc4)C[C@H]3C2)nc2ccccc21
ZINC000558477778	Cn1c(CCN2C[C@@H]3CCN(Cc4ccccc4)C[C@H]3C2)nc2ccccc21
ZINC000578101381	FC(F)n1c(CN2C[C@@H]3CCN(Cc4ccccc4)C[C@@H]3C2)nc2ccccc21
ZINC000578101382	FC(F)n1c(CN2C[C@H]3CCN(Cc4ccccc4)C[C@@H]3C2)nc2ccccc21

Compound ID	Smiles
ZINC000583232307	Cn1c(CN2C[C@H]3CCN(Cc4ccccc4)C[C@H]3C2)nc2cc(Cl)ccc21
ZINC000595550943	N#Cc1ccc(CN2CCC(Cc3nc4ccccc4[nH]3)CC2)cc1
ZINC000595552252	N#Cc1cccc(CN2CCC(Cc3nc4ccccc4[nH]3)CC2)c1
ZINC000660852701	NC(=O)c1ccc(CN2CCC(Cc3nc4ccccc4[nH]3)CC2)cc1
ZINC000660857670	c1ccc2[nH]c(CC3CCN(Cc4ccc5c[nH]nc5c4)CC3)nc2c1
ZINC000681530378	CC1(C(=O)N2CC(c3nc4ccccc4[nH]3)C2)CCN(Cc2ccccc2)CC1
ZINC000685850863	CCn1c(CN2C[C@H]3CCN(Cc4ccccc4)C[C@@H]3C2)nc2ccccc21
ZINC000685850865	CCn1c(CN2C[C@@H]3CN(Cc4ccccc4)CC[C@H]3C2)nc2ccccc21
ZINC000776101081	CCn1c(CNC(=O)C2(C)CCN(Cc3ccccc3)CC2)nc2ccccc21
ZINC001460279169	Fc1cccc(F)c1CN1CCC(Cc2nc3ccccc3[nH]2)CC1
ZINC001559932821	N#Cc1cc(F)ccc1CN1CCC(Cc2nc3ccccc3[nH]2)CC1
ZINC001643530497	Fc1ccc(CN2CCC(Cc3nc4ccccc4[nH]3)CC2)c(F)c1
ZINC001643530535	Fc1ccc(CN2CCC(Cc3nc4ccccc4[nH]3)CC2)cc1F
ZINC001643530677	Cc1ccc(CN2CCC(Cc3nc4ccccc4[nH]3)CC2)cc1F
ZINC001659113360	FCc1ccc(CN2CCC(Cc3nc4ccccc4[nH]3)CC2)cc1
BACE-1 Target	
ZINC000047304344	O=C(C1CCN(Cc2ccccc2)CC1)N1CCC[C@H](c2nc3ccccc3[nH]2)C1
ZINC000057153401	O=C(C1CCN(Cc2ccccc2)CC1)N1CCC[C@H]1c1nc2ccccc2[nH]1
ZINC000103265237	Cn1c(CC2CCN(C(=O)c3ccccc3)CC2)nc2cc(C(=O)Nc3cccnc3)ccc21
ZINC000142264658	Cc1ccc2nc([C@@H]3CCCN3C(=O)C3CCN(Cc4ccccc4)CC3)[nH]c2c1
ZINC000157562106	C[C@H](NC(=O)C1(C)CCN(Cc2ccccc2)CC1)c1nc2ccccc2[nH]1
ZINC000157878666	CC1(C(=O)NCc2nc3ccccc3[nH]2)CCN(Cc2ccccc2)CC1
ZINC000163487758	Cn1c(CCNC(=O)C2(C)CCN(Cc3ccccc3)CC2)nc2ccccc21
ZINC000184835020	CC1(C(=O)NCc2nc3cc(F)ccc3[nH]2)CCN(Cc2ccccc2)CC1
ZINC000198140355	O=C(NCc1nc2ccccc2[nH]1)C1CCN(C(=O)c2ccc(F)cc2F)CC1
ZINC000274466734	COc1ccc2c(c1)nc(CNC(=O)C1CCN(Cc3ccccc3)CC1)n2C
ZINC000415134114	Cn1c(CNCC2(N)CCN(Cc3ccccc3)CC2)nc2ccccc21
ZINC000415135077	Cn1c(CNCC2(N)CCN(Cc3ccccc3)CC2)nc2ccc(Cl)cc21
ZINC000415137470	Cn1c(CNCC2(N)CCN(Cc3ccccc3)CC2)nc2cc(Cl)ccc21
ZINC000415139881	CCCn1c(CNCC2(N)CCN(Cc3ccccc3)CC2)nc2ccccc21
ZINC000508233008	Cc1ccc2nc([C@H]3CCCN(C(=O)C4CCN(Cc5ccccc5)CC4)C3)[nH]c2c1
ZINC000512110306	CCC1(C(=O)NCCc2nc3ccc(F)cc3[nH]2)CCN(C(=O)c2ccccc2)CC1
ZINC000518079309	CCn1c([C@@H](C)NC(=O)C2CCN(Cc3ccccc3)CC2)nc2ccccc21
ZINC000541572808	Cn1c(CCNC(=O)C2(C)CCN(Cc3ccccc3)CC2)nc2ccc(F)cc21
ZINC000543434141	Cn1c(CCNC(=O)C2(C)CCN(Cc3ccccc3)CC2)nc2c(F)cccc21
ZINC000552367493	Cc1ccc(C(=O)N2CCC(Cc3nc4ccccc4[nH]3)CC2)cc1
ZINC000558477775	Cn1c(CCN2C[C@H]3CN(Cc4ccccc4)CC[C@H]3C2)nc2ccccc21
ZINC000558477776	Cn1c(CCN2C[C@H]3CCN(Cc4ccccc4)C[C@@H]3C2)nc2ccccc21
ZINC000568755665	O=C(c1cccc2cnccc12)N1CCC(Cc2nc3ccccc3[nH]2)CC1
ZINC000576196756	c1ccc(CN2CC[C@@H]3CN(Cc4nc5ccccc5[nH]4)C[C@H]3C2)cc1
ZINC000577410686	Cc1cccc(C)c1C(=O)N1CCC(Cc2nc3ccccc3[nH]2)CC1
ZINC000595551328	N#Cc1cccc(CN2CCC(Cc3nc4ccccc4[nH]3)CC2)c1F
ZINC000595551587	N#Cc1cc(CN2CCC(Cc3nc4ccccc4[nH]3)CC2)ccc1F
ZINC000600518437	CN(Cc1nc2ccccc2n1C)C(=O)C1CCN(Cc2ccccc2)CC1
ZINC000614968635	O=C(c1ccc(CO)cc1)N1CCC(Cc2nc3ccccc3[nH]2)CC1
ZINC000660852701	NC(=O)c1ccc(CN2CCC(Cc3nc4ccccc4[nH]3)CC2)cc1
ZINC000660856112	NC(=O)[C@@H](c1ccccc1)N1CCC(Cc2nc3ccccc3[nH]2)CC1
ZINC000682003918	CC1(C(=O)NCc2nc3ccc(Cl)cc3[nH]2)CCN(Cc2ccccc2)CC1
ZINC000686762538	Cc1ccc2nc(CC3(N)CCN(Cc4ccccc4)CC3)[nH]c2c1
ZINC000761586144	O=C(C1CCN(C2=NS(=O)(=O)c3ccccc32)CC1)N1CC(c2nc3ccccc3[nH]2)C1
ZINC000832191421	Nc1ccc(C(=O)N2CCC(Cc3nc4ccccc4[nH]3)CC2)cc1
ZINC000832192390	NCc1cccc(C(=O)N2CCC(Cc3nc4ccccc4[nH]3)CC2)c1
ZINC001643530497	Fc1ccc(CN2CCC(Cc3nc4ccccc4[nH]3)CC2)c(F)c1
ZINC001643530535	Fc1ccc(CN2CCC(Cc3nc4ccccc4[nH]3)CC2)cc1F
ZINC001654813914	COc1ccc(CN2CCC(Cc3nc4ccccc4[nH]3)CC2)cc1
ZINC001659113360	FCc1ccc(CN2CCC(Cc3nc4ccccc4[nH]3)CC2)cc1
ZINC001828853049	Cc1cc2nc(C(=O)N3CCCC[C@@H]3C3CCN(C(=O)c4cc(O)ccc4F)CC3)[nH]c2cc1C

2.2. Protein preparation and receptor grid generation.

In this study, the three-dimensional X-ray crystal structures of two key proteins implicated in Alzheimer's disease, human β-secretase 1 (BACE-1, PDB ID: 2WJO) and acetylcholinesterase (AChE, PDB ID:4EY7), were retrieved from the RCSB Protein Data Bank. The selected structures were of high resolution and co-crystallized with inhibitors,

ensuring accurate representation of the binding sites. The proteins were prepared using the Protein Preparation Wizard in Maestro (Schrödinger Release 2021-2), which involved the assignment of correct bond orders, the addition of missing hydrogen atoms, the optimization of hydroxyl, Asn, Gln, and His orientations, and the assignment of protonation states appropriate for pH 7.0. Water molecules beyond 5 Å from the binding sites were removed unless involved in critical hydrogen bonding interactions. Following these steps, the protein structures were energy minimized using the OPLS_2005 force field until convergence was reached with a root-mean-square deviation (RMSD) threshold of 0.30 Å, ensuring stability and readiness for docking [42]

After protein preparation, receptor grid generation was performed to define the active binding sites. The grid box was centered on the co-crystallized ligand to ensure accurate positioning of the ligand within the catalytic pocket. Grid dimensions were adjusted to fully accommodate diverse ligand sizes without steric clashes, typically covering a region of 20 $Å^3$. Molecular docking was then conducted using the Glide module in Maestro, following a hierarchical protocol that included High-Throughput Virtual Screening (HTVS), Standard Precision (SP), and Extra Precision (XP) modes. The HTVS mode allowed rapid initial screening of all 431 benzimidazole derivatives. Compounds with good scores were passed to the SP mode for refined docking based on improved sampling and scoring. Finally, the top-scoring compounds were docked in XP mode, which applied enhanced sampling, energy weighting, and penalization of false positives using the GlideScore scoring function. This stepwise approach allowed efficient filtering of potent molecules while maintaining accuracy in docking predictions [43,44].

2.3. ADMET study.

To evaluate the pharmacokinetic and toxicity profiles of the selected benzimidazole derivatives, a comprehensive *in silico* ADMET (Absorption, Distribution, Metabolism, Excretion, and Toxicity) analysis was performed using QikProp (Schrödinger, Release 2021) and Discovery Studio (BIOVIA, 2021)[45, 34]. Initially, all ligands were energy minimized and prepared using the LigPrep module with the OPLS_2005 force field. These optimized structures were then further refined in Discovery Studio using the CHARMM (Chemistry at Harvard Macromolecular Mechanics) force field to ensure compatibility with the ADMET descriptor models [46]. QikProp was used to predict several key pharmacokinetic properties, such as CNS activity score, blood-brain barrier permeability (QPlogBB), octanol-water partition coefficient (QPlogPo/w), aqueous solubility (QPlogS), human oral absorption (%HOA), Caco-2 and MDCK cell permeability (QPPCaco and QPPMDCK), hERG inhibition potential (QPlogHERG), and serum protein binding (QPlogKhsa). These predictions provided insight into the drug-likeness and CNS accessibility of each compound.

In addition to pharmacokinetic evaluation, toxicity predictions were conducted using the ADMET descriptors protocol in Discovery Studio. This included assessment of blood-brain barrier level (on a scale of 0–4), solubility level, absorption potential, CYP2D6 inhibition (to assess drug–drug interaction risk), hepatotoxicity prediction, and plasma protein binding classification. Furthermore, genotoxicity and safety margins were evaluated through predicted mutagenicity, rat acute oral toxicity (LD_{50}), chronic oral toxicity (TD50), and aquatic toxicity (EC_{50} in Daphnia). The majority of lead compounds showed non-mutagenic profiles with good BBB permeability and high intestinal absorption, making them suitable candidates for CNS-targeted therapies. Compounds also demonstrated acceptable protein binding and solubility

profiles, with some variation in predicted cardiotoxicity risk based on hERG scores. This detailed ADMET profiling helped in shortlisting the most promising benzimidazole derivatives for further development as dual-target anti-Alzheimer agents.

2.4. Structure-based virtual screening.

Virtual screening was employed to identify potential inhibitors of acetylcholinesterase (AChE) and beta-site amyloid precursor protein cleaving enzyme 1 (BACE-1). However, given the large dataset of compounds obtained from the initial screening, it was impractical to directly subject all of them to molecular docking in extra precision (XP) mode. To refine the dataset and ensure computational efficiency, a structure-based virtual screening (SBVS) approach was implemented to filter the compounds based on their docking scores. SBVS is an effective computational method that prioritizes compounds with higher binding affinities and favorable interactions with target proteins, thereby narrowing the candidate pool for further investigation.

The SBVS process utilized the high-throughput virtual screening (HTVS) docking protocol to streamline the identification of promising inhibitors. To conduct the molecular docking studies, the Grid-based Ligand Docking with Energetics (GLIDE) software was used. GLIDE is a widely recognized docking tool that uses a hierarchical filtering approach to screen ligand-receptor interactions efficiently. The software first explores potential ligand binding poses within the receptor's active site through an extensive sampling process. It then refines the docking results by progressively applying more accurate scoring functions. This is achieved by representing the receptor's shape and properties using a set of grid-based fields, which facilitate the precise evaluation of ligand binding affinity.

GLIDE's docking procedure is designed to accommodate the flexibility of both ligands and receptors, which is crucial in achieving accurate docking results. The software employs an extensive conformational search algorithm to explore different possible orientations of the ligands. Additionally, it incorporates a heuristic screening mechanism that quickly discards unfavorable ligand conformations that do not meet the docking criteria. This dual approach ensures that only the most promising ligand-receptor interactions are retained for further evaluation.

To further refine the dataset, additional screening criteria were applied based on QikProp predictions, Lipinski's Rule of Five, and reactive functional group filtering. These parameters help in assessing the drug-likeness, pharmacokinetic properties, and potential toxicity of the molecules. Out of an initial set of 431 unique molecules (comprising 1784 structural variations), 422 molecules (with a total of 1677 structural variations) were found to meet the preliminary screening criteria. These selected compounds were then subjected to SBVS using the HTVS docking protocol.

Following this round of screening, 42 molecules (representing 208 to 261 structural variations) were shortlisted for docking in standard precision (SP) mode. The SP mode provides a more refined docking evaluation by considering additional energetic and geometric constraints. This step further reduces the number of candidates by eliminating those with suboptimal binding affinities or unfavorable interactions with the target proteins.

From this subset, four compounds demonstrated superior docking performance and were subsequently selected for the highest level of docking accuracy, XP mode. The XP docking protocol applies the most stringent evaluation criteria, incorporating advanced scoring functions to assess ligand binding with maximal precision.

In the molecular docking process performed using the Glide software, all three docking modes: High Throughput Virtual Screening (HTVS), Standard Precision (SP), and Extra Precision (XP) employ a grid-based ligand docking algorithm paired with an empirical scoring function. This approach involves a hierarchical sequence of filtering and refinement steps to optimize ligand-receptor interactions. Specifically, the algorithm samples multiple ligand conformations and orientations, strategically places them within a predefined receptor grid representing the target protein's active site, and subsequently evaluates each pose based on interaction energies and geometric compatibility. This structured procedure ensures accurate prediction of binding affinities while accommodating varying levels of computational rigor across the three modes.

3. Results and Discussion

3.1. Structure-based virtual screening.

The virtual screening process employed in this study involved multiple stages of filtering and docking to identify potential inhibitors of acetylcholinesterase (AChE) and beta-site amyloid precursor protein cleaving enzyme 1 (BACE-1), as depicted in Figure 2. Initially, a total of 431 unique molecules, corresponding to 1784 structural variations, were subjected to an initial filtering process. This was based on key drug-likeness parameters, including QuickProp analysis, Lipinski's Rule of Five, and reactive functional group filtering, ensuring that only compounds with favorable pharmacokinetic properties and minimal toxicity were considered for further evaluation.

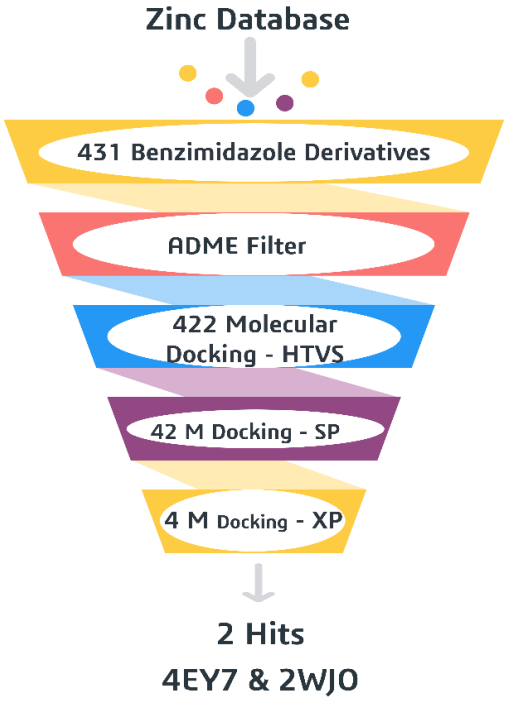

Figure 2. Workflow for virtual screening of benzimidazole derivatives.

After applying these filters, 422 molecules (with 1677 structural variations) were selected for structure-based virtual screening (SBVS) using the high-throughput virtual screening (HTVS) docking protocol (Supplementary file Table S2). This initial docking step was conducted to rapidly screen a large number of compounds and eliminate those with poor

binding affinity to the target receptors. The chemical structure and compound ID for the final selected molecules are shown in Table 2.

Table 2. The chemical structures of six molecules submitted for XP-docking.

Compound ID	Chemical structure
ZINC000558477778	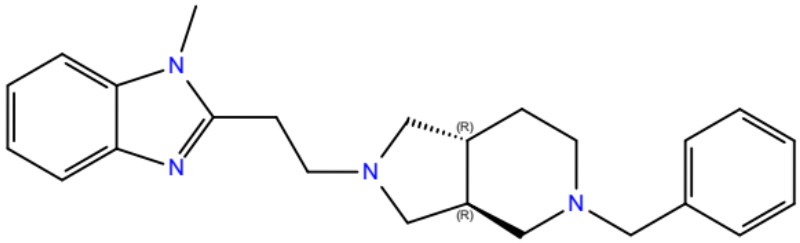
ZINC000558477776	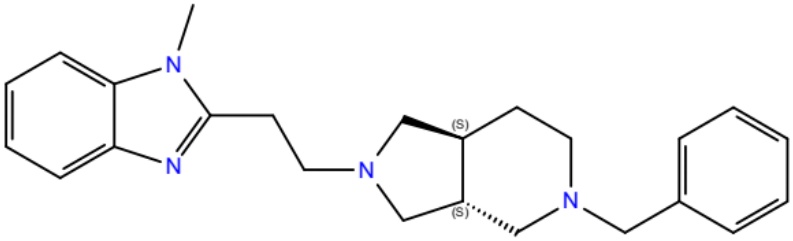
ZINC000558477775	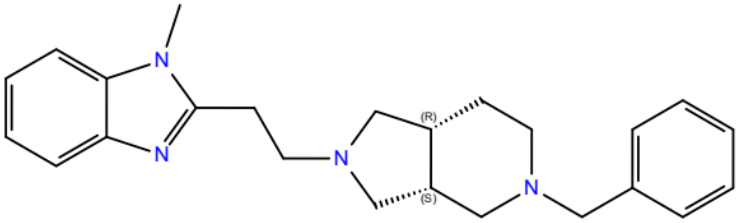
ZINC000558477777	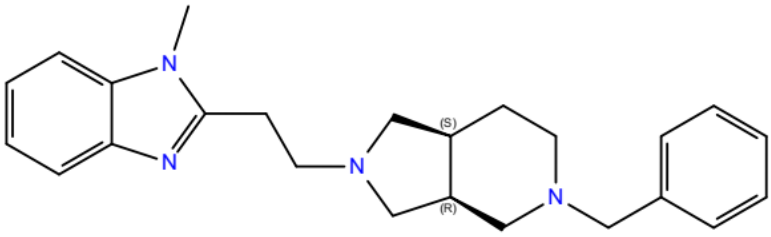
ZINC000614968635	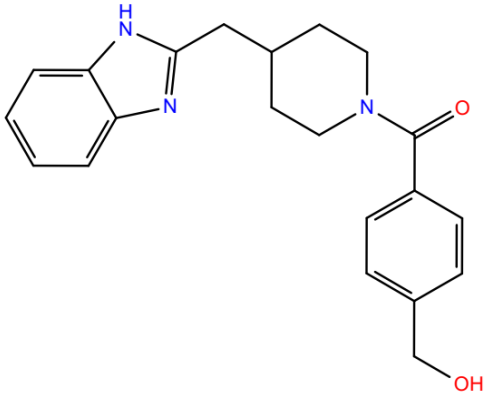

Compound ID	Chemical structure
ZINC000552367493	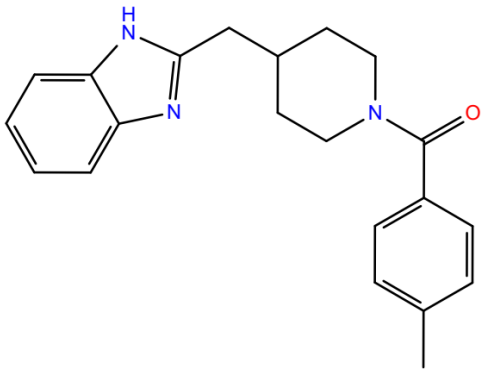

3.2. Selection of lead compounds from HTVS and SP docking.

Following HTVS docking, the best-performing molecules were further refined through standard precision (SP) docking. This step provided a more detailed analysis of ligand-receptor interactions, enabling the selection of high-affinity compounds for the final docking phase. For AChE (PDB: 4EY7) 42 molecules, corresponding to 261 structural variations, were selected based on their superior docking scores and favorable binding interactions. That of for BACE-1 (PDB: 2WJO): 41 molecules, corresponding to 208 structural variations, were shortlisted for further docking studies. From these 41/42 compounds, four were ultimately chosen for extra-precision (XP) docking, which employs the most stringent scoring criteria and advanced algorithms to evaluate ligand binding with maximum accuracy.

3.3. XP docking results and binding affinities.

The XP docking phase provided crucial insights into the binding strengths of the selected molecules. The top-ranked compounds demonstrated significant binding affinities towards both AChE and BACE-1, as reflected in their XP GlideScores (GScore). The XP docking scores, which indicate the estimated binding free energy (lower values signify stronger binding), are summarized in Table 3.

Table 3. Selected four XP Docking Scores against AChE and BACE-1.

AChE 4EY7 - PDB		**BACE-1 2WJO - PDB**	
Compound ID	**XP docking score**	**Compound ID**	**XP docking score**
ZINC000558477778	-19.087	ZINC000614968635	-7.43
ZINC000558477776	-18.646	ZINC000558477775	-7.198
ZINC000558477775	-18.455	ZINC000552367493	-6.398
ZINC000558477777	-18.248	ZINC000558477776	-5.912

The results indicate that the ZINC000558477778 molecule exhibited the highest binding affinity for AChE, achieving an XP GlideScore of -19.087, while ZINC000614968635 showed the best binding affinity towards BACE-1 with an XP GlideScore of -7.43.

Additionally, ZINC000558477776 and ZINC000558477775 displayed strong interactions with both targets, highlighting their potential as dual inhibitors. These molecules exhibited docking scores of -18.646 (AChE) and -7.198 (BACE-1), respectively. The presence of common molecules with strong binding affinities towards both enzymes suggests that these compounds could serve as promising dual inhibitors of AChE and BACE-1, which is crucial in the search for effective Alzheimer's disease treatments.

The selection of AChE and BACE-1 as target proteins was based on their critical and complementary roles in the pathogenesis of Alzheimer's disease (AD). Acetylcholinesterase

(AChE) hydrolyzes the neurotransmitter acetylcholine in the synaptic cleft, and excessive AChE activity is associated with reduced cholinergic transmission, a hallmark of cognitive impairment in AD. Therefore, AChE inhibition is a well-established symptomatic treatment strategy for improving memory and cognition. On the other hand, beta-site amyloid precursor protein cleaving enzyme 1 (BACE-1) plays a key role in the amyloidogenic pathway by initiating the cleavage of amyloid precursor protein (APP), which leads to the formation of amyloid-beta (Aβ) peptides. These peptides aggregate to form plaques that contribute to neuronal toxicity and AD progression. Inhibition of BACE-1 has been proposed as a disease-modifying approach aimed at reducing Aβ burden and slowing neurodegeneration.

Thus, targeting both AChE and BACE-1 simultaneously offers a dual-action therapeutic strategy that provides symptomatic relief (via AChE inhibition) and slows disease progression (via BACE-1 inhibition). The use of these two proteins in docking studies reflects a rational approach for identifying multi-target-directed ligands (MTDLs) for Alzheimer's therapy.

3.4. Molecular interaction insights.

To identify potential inhibitors for AChE and BACE-1, a hierarchical docking approach was implemented using HTVS, SP docking, and extra precision (XP) docking. This approach ensured the selection of highly potent compounds based on their binding affinity and molecular interactions. Based on SP docking results, four molecules from each target were selected for XP docking, which provided the most accurate estimation of ligand-binding affinities. The XP docking scores for the top four compounds against AChE ranged from -18.248 to -19.087, while for BACE-1, they ranged from -5.912 to -7.43, indicating strong binding interactions.

3.4.1. Molecular docking interactions with AChE.

Acetylcholinesterase is a key enzyme responsible for breaking down acetylcholine (ACh) at synaptic junctions. Inhibiting AChE can help improve cholinergic signaling, a crucial strategy in treating Alzheimer's disease. The selected compounds showed strong docking scores, highlighting their potential as effective inhibitors (Figure 3).

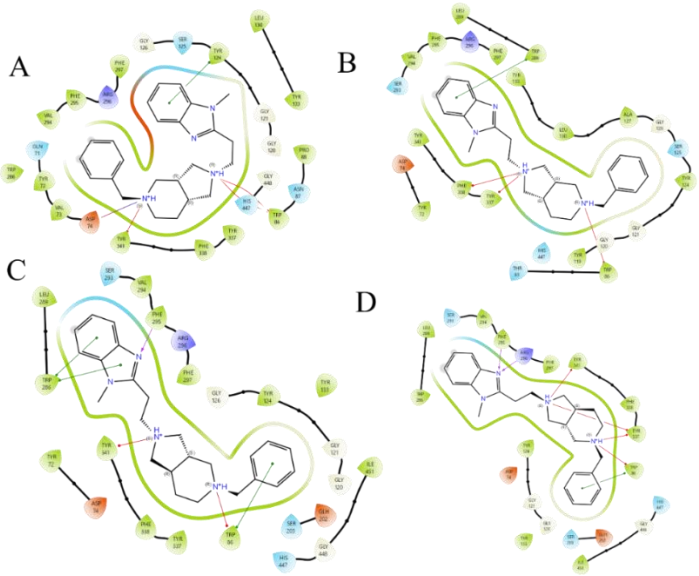

Figure 3. The 2D binding mode of **(A)** ZINC000558477778; **(B)** ZINC000558477776; **(C)** ZINC000558477775; **(D)** ZINC000558477777 in the active site of the AChE enzyme.

Among the AChE inhibitors, ZINC000558477778 exhibited the highest XP docking score of -19.087, indicating its strong binding affinity. It interacted with Asp 74 via a salt bridge (4.43 Å), pi-cation interactions with Tyr 341 (3.34 Å) and Trp 84 (3.97 Å, 4.42 Å), and pi-pi stacking with Tyr 124 (5.41 Å). These interactions suggest that this compound binds efficiently at both the catalytic active site (CAS) and peripheral anionic site (PAS), making it a strong candidate for dual inhibition of AChE activity and amyloid-beta (Aβ) aggregation.

The second-best AChE inhibitor, ZINC000558477776, had an XP docking score of -18.646 and displayed pi-pi stacking interactions with Trp 286 (4.21 Å), pi-cation interactions with Phe 338 (4.21 Å), Tyr 337 (4.11 Å), and Trp 86 (3.64 Å). These interactions stabilized the molecule within the enzyme's active site, enhancing its inhibitory effect. ZINC000558477775, with an XP docking score of -18.455, formed multiple pi-pi stacking interactions with Trp 286 (4.32 Å, 4.16 Å) and Trp 86 (4.08 Å). It also exhibited hydrogen bonding with Phe 295 (2.60 Å) and pi-cation interactions with Tyr 341 (3.09 Å) and Trp 86 (4.56 Å), contributing to a highly stable AChE-ligand complex. ZINC000558477777, with an XP docking score of -18.248, interacted via hydrogen bonds with Phe 295 (2.35 Å) and Arg 296 (2.70 Å), along with pi-cation interactions with Tyr 341 (3.86 Å), Tyr 337 (6.37 Å, 4.47 Å), and Trp 86 (4.70 Å). These interactions enhanced its binding stability, reinforcing its potential as an AChE inhibitor.

3.4.2. Molecular docking interactions with BACE-1.

Beta-secretase 1 (BACE-1) plays a crucial role in the cleavage of the amyloid precursor protein (APP), leading to the formation of amyloid-beta plaques, a major factor in Alzheimer's disease progression. The selected compounds exhibited moderate to strong docking scores, indicating effective inhibition of the enzyme (Figure 4).

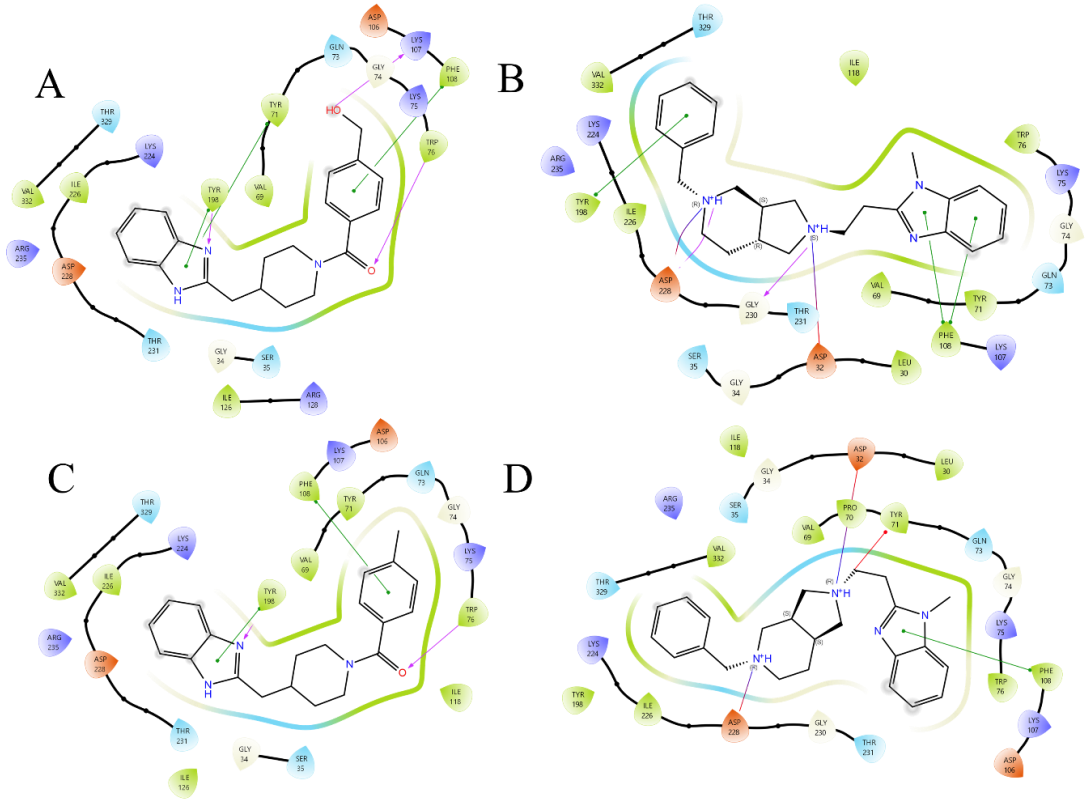

Figure 4. The 2D binding mode of **(A)** ZINC000614968635; **(B)** ZINC000558477775; **(C)** ZINC000552367493; **(D)** ZINC000558477776 in the active site of the BACE-1 enzyme.

ZINC000614968635, the top-scoring inhibitor for BACE-1, had an XP docking score of -7.43, indicating a strong binding affinity. It formed pi-pi stacking interactions with Tyr 198 (5.27 Å) and Tyr 71 (5.19 Å), along with hydrogen bonds with Tyr 198 (2.05 Å), Lys 107 (2.07 Å), and Trp 76 (2.04 Å). These interactions suggest that this molecule is efficiently positioned within the active site, stabilizing the enzyme-ligand complex and hindering BACE-1 activity. ZINC000558477775, with an XP docking score of -7.198, displayed pi-pi stacking interactions with Tyr 198 (5.22 Å) and Phe 108 (4.92 Å, 5.15 Å), as well as salt bridge interactions with Asp 228 (3.03 Å) and Asp 32 (3.88 Å). The presence of hydrogen bonds with Asp 228 (2.38 Å) and Gly 230 (2.23 Å) further strengthened its binding affinity. ZINC000552367493, with an XP docking score of -6.398, exhibited pi-pi stacking interactions with Tyr 198 (5.49 Å) and Phe 108 (4.96 Å), along with hydrogen bonds with Tyr 198 (2.25 Å) and Trp 76 (2.06 Å). These interactions provided strong stabilization within the BACE-1 active site, supporting its potential role as an effective inhibitor. ZINC000558477776, with an XP docking score of -5.912, formed salt bridge interactions with Asp 228 (3.02 Å) and Asp 32 (4.35 Å), along with pi-cation interactions with Tyr 71 (5.68 Å) and pi-pi stacking with Phe 108 (4.96 Å). Although its docking score was lower than those of the other candidates, its strong electrostatic and hydrophobic interactions still make it a viable inhibitor.

The molecular docking results indicate that the selected compounds exhibit high binding affinity and strong interactions with both AChE and BACE-1. For AChE, the XP docking scores ranged from -18.248 to -19.087, indicating strong binding interactions at both the CAS and PAS sites. The presence of pi-cation and pi-pi stacking interactions with key residues such as Trp 86, Tyr 341, and Trp 286, along with hydrogen bonding and salt bridge formations, contributed to high stability within the active site. These findings suggest that these molecules have potential as multitarget inhibitors, offering both cholinergic enhancement and anti-amyloid properties for Alzheimer's disease treatment. For BACE-1, the XP docking scores ranged from -5.912 to -7.43, with all four selected compounds forming significant pi-pi stacking, hydrogen bonding, and salt bridge interactions with key catalytic residues. The top-scoring compounds, ZINC000614968635 and ZINC000558477775, demonstrated strong inhibitory potential, making them promising candidates for reducing amyloid-beta production.

The findings suggest that the selected compounds possess dual-target inhibition potential, effectively blocking AChE to enhance neurotransmission while inhibiting BACE-1 to reduce amyloid plaque formation. Their high docking scores, strong molecular interactions, and multitarget potential make them valuable candidates for further drug development. Future studies should focus on molecular dynamics simulations, ADME analysis, and *in vitro* validation to confirm their stability, bioavailability, and therapeutic efficacy before proceeding to preclinical and clinical trials.

To validate the accuracy of the molecular docking protocol, the native ligand Donepezil for AChE and the co-crystallized ligand for BACE-1 (PDB ID: 2WJO) were redocked into their respective active sites. The docking scores obtained were –12.542 kcal/mol for Donepezil in AChE and –6.29 kcal/mol in BACE-1, while the 2WJO ligand showed scores of –8.943 kcal/mol in AChE and –6.68 kcal/mol in BACE-1. These results, along with the interaction diagrams generated during docking, confirm that the proteins were correctly prepared and that the defined active sites are suitable for ligand binding. The consistency between observed and redocked binding poses reinforces the reliability of the docking strategy applied in this study.

In this study, the Ramachandran plots for AChE and BACE-1 were generated and presented in Figure 5, confirming that the proteins used are structurally sound. The plots

showed that a high percentage of residues lie within the most favored regions, with minimal outliers, indicating that the protein models are suitable for downstream molecular docking and simulation analyses.

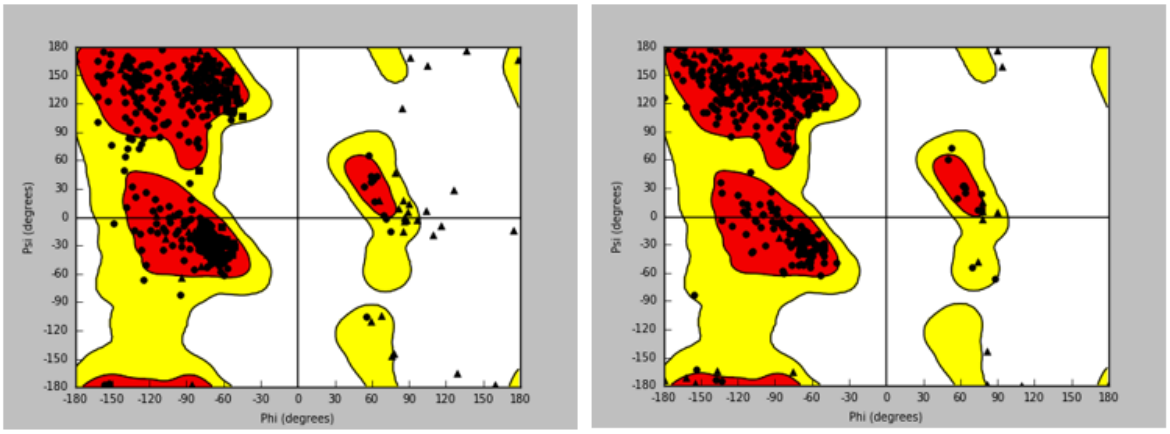

(a) 4EY7 (b) 2WJO

Figure 5. Ramachandran plot for AChE and BACE-1.

3.5. ADMET prediction.

The ADME (Absorption, Distribution, Metabolism, and Excretion) properties of the selected molecules were evaluated using the QikProp module in Schrödinger and presented in Table 4. This analysis helps determine the drug-likeness and pharmacokinetic feasibility of the compounds for potential therapeutic use. Various parameters, including CNS activity, human oral absorption (HOA), permeability (QPPCaco, QPPMDCK), lipophilicity (QPlogPo/w), solubility (QPlogS), blood-brain barrier penetration (QPlogBB), and potential cardiotoxicity (QPlogHERG), were analyzed to assess the pharmacokinetic suitability of the compounds.

Table 4. ADME analysis of the top 06 hits using QikProp.

Compound ID	CNS	HOA	%HOA	QPPCaco	QPPMDCK	QPlogBB	QPlogHERG	QPlogKhsa	QPlogPo/w	QPlogS	accept HB	donor HB	Rule Of Five	Rule Of Three
ZINC000558477778	2	3	100	347.833	193.369	0.785	-8.006	0.693	4.259	-3.721	5.5	0	0	0
ZINC000558477776	2	3	100	337.146	186.955	0.769	-8.048	0.695	4.256	-3.761	5.5	0	0	0
ZINC000558477775	2	3	100	381.381	213.604	0.827	-8.084	0.719	4.348	-3.86	5.5	0	0	0
ZINC000558477777	2	3	100	356.519	198.593	0.799	-7.918	0.673	4.214	-3.623	5.5	0	0	0
ZINC000614968635	-2	3	95.968	581.184	275.17	-1.063	-6.123	0.337	3.338	-5.236	6.2	2	0	0
ZINC000552367493	0	3	100	1918.14	1000.254	-0.365	-5.956	0.72	4.411	-5.896	4.5	1	0	1

The CNS activity score is an essential factor for drugs targeting neurodegenerative diseases like Alzheimer's disease. The top four molecules (ZINC000558477778, ZINC000558477776, ZINC000558477775, and ZINC000558477777) exhibited a CNS score of 2, indicating excellent penetration into the central nervous system (CNS). This is highly favorable for drugs aimed at treating CNS disorders. In contrast, ZINC000614968635 and ZINC000552367493 had lower CNS scores (-2 and 0, respectively), suggesting limited BBB penetration and, thus, reduced effectiveness for CNS-targeted therapies.

Human oral absorption (HOA) and permeability parameters provide insights into how well a compound can be absorbed into the bloodstream. All selected molecules showed high oral absorption (HOA value of 3), with a percentage of 95–100%, indicating their strong

potential for oral bioavailability. Additionally, Caco-2 permeability (QPPCaco) values confirmed good absorption potential, with ZINC000552367493 exhibiting the highest value (1918.14), followed by ZINC000614968635 (581.184). These high permeability scores suggest efficient intestinal absorption, a critical factor for drug efficacy. Similarly, MDCK permeability (QPPMDCK) values, which predict drug transport across cell membranes, further supported these findings, with ZINC000552367493 (1000.254) exhibiting the highest permeability.

The ability of a drug to cross the blood-brain barrier (BBB) is essential for CNS-active drugs. The QPlogBB values indicate BBB penetration potential, with values above 0.3 suggesting good permeability. The top four molecules showed favorable QPlogBB values ranging from 0.769 to 0.827, supporting their potential effectiveness in neurological disorders. However, ZINC000614968635 (-1.063) and ZINC000552367493 (-0.365) had significantly lower QPlogBB values, indicating their limited ability to penetrate the CNS and potentially making them less suitable for neurological applications.

The binding affinity to human serum albumin (HSA), measured by QPlogKhsa, affects drug distribution and availability in the bloodstream. Most selected molecules had QPlogKhsa values between 0.673 and 0.72, suggesting moderate to strong plasma protein binding, which can enhance drug stability and prolong circulation time. ZINC000614968635, with a lower QPlogKhsa value (0.337), may have a shorter half-life, affecting its bioavailability.

Lipophilicity and aqueous solubility are crucial for drug absorption and distribution. The octanol/water partition coefficient (QPlogPo/w) values for all selected molecules were within the optimal range, between 3.338 and 4.411, indicating good membrane permeability. However, solubility (QPlogS) values showed that ZINC000614968635 (-5.236) and ZINC000552367493 (-5.896) had lower aqueous solubility, which could pose challenges for formulation and bioavailability.

A critical concern in drug development is hERG inhibition (QPlogHERG), which predicts the potential for cardiotoxicity. A QPlogHERG value below -5 suggests a high risk of cardiotoxicity. Unfortunately, the top four AChE inhibitors (ZINC000558477778, ZINC000558477776, ZINC000558477775, and ZINC000558477777) exhibited values between -7.918 and -8.084, indicating a significant risk. Similarly, ZINC000614968635 (-6.123) and ZINC000552367493 (-5.956) also showed potential cardiotoxicity risks, though slightly less severe.

Finally, adherence to Lipinski's Rule of Five and Rule of Three is essential for evaluating drug-likeness. All selected compounds complied with Lipinski's Rule of Five, making them strong candidates for oral drug development. However, ZINC000552367493 violated one condition of the Rule of Three, indicating that it may require further optimization for early drug discovery. The ADME profiling of the selected XP docking hits revealed promising drug-like characteristics, particularly for the four AChE inhibitors (ZINC000558477778, ZINC000558477776, ZINC000558477775, and ZINC000558477777). These compounds demonstrated excellent CNS penetration, high oral absorption, good permeability, and optimal lipophilicity, making them strong candidates for further development. However, their hERG inhibition scores indicate a potential risk for cardiotoxicity, necessitating further toxicity assessments and structural modifications. On the other hand, ZINC000614968635 and ZINC000552367493 exhibited high permeability and strong oral absorption. Still, their poor CNS penetration and moderate cardiotoxicity risk suggest they may be better suited for non-CNS-targeted drug development.

Figure 6 illustrates the correlation between the polar surface area (PSA) and lipophilicity (AlogP) for the selected benzimidazole derivatives, highlighting the 95% and 99% confidence ellipses corresponding to the blood-brain barrier (BBB) and human intestinal absorption (HIA) models. These ellipses represent the likelihood that molecules will cross the BBB and be absorbed in the human intestine. All the molecules are in the eclipse and near the donepezil.

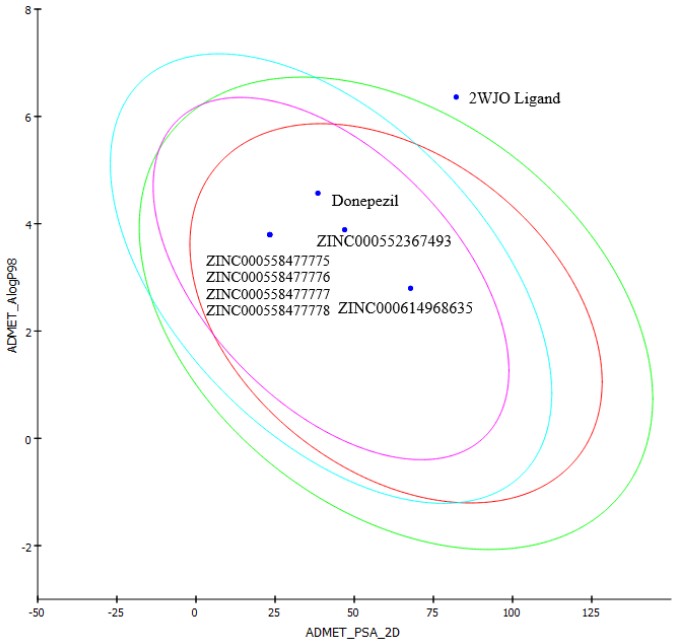

Figure 6. Plot of PSA versus A log P for selected molecules showing 95% and 99% confidence limit ellipses corresponding to the blood–brain barrier (BBB) and human intestinal absorption (HIA) models.

From the ADMET predictions presented in Table 5, it is observed that most benzimidazole derivatives (ZINC000558477778, ZINC000558477776, ZINC000558477775, ZINC000558477777, and ZINC000552367493) exhibit high BBB permeability (level 1), similar to the reference drug donepezil. This suggests their potential for central nervous system (CNS) activity. One compound (ZINC000614968635) showed medium BBB permeability (level 2), whereas the 2WJO Ligand displayed very low BBB permeability (level 4), indicating limited CNS penetration.

Table 5. Predicted ADMET for benzimidazole derivatives and reference drug.

Compound No	BBB level	Solubility level	Absorption level	CYP2D6 prediction	Hepatotoxic prediction	PPB prediction
ZINC000558477778	1	2	0	FALSE	FALSE	TRUE
ZINC000558477776	1	2	0	FALSE	FALSE	TRUE
ZINC000558477775	1	2	0	FALSE	FALSE	TRUE
ZINC000558477777	1	2	0	FALSE	FALSE	TRUE
ZINC000614968635	2	3	0	FALSE	FALSE	TRUE
ZINC000552367493	1	2	0	FALSE	TRUE	TRUE
Donepezil	1	2	0	FALSE	FALSE	TRUE
2WJO Ligand	4	1	2	FALSE	TRUE	TRUE

ADMET descriptors. For good absorption through BBB , level required , 0 = very high, 1 = high, 2 = medium, 3 = low, 4 = very low; Solubility indicates molar solubility of the drug, where 1 = very low solubility, 2 = low solubility, 3 = good solubility, and 4 = optimal solubility; Absorption level, 0 = good, 1 = moderate, 2 = poor, 3 = very poor; CYP2D6 (cytochrome P2D6) descriptor determines inhibitory effect by predicted classes as TRUE = inhibitor, FALSE = non-inhibitor; Hepatotoxicity determines the toxicity of a drug by predicted classes: TRUE = hepatotoxic, FALSE = non-hepatotoxic; PBB (plasma protein binding) determines binding of the drug; FALSE means less than 90% binding, TRUE means more than 90% binding.

Regarding solubility, most compounds demonstrated low solubility (level 2), while ZINC000614968635 exhibited good solubility (level 3). The 2WJO Ligand had the lowest solubility (level 1), which may limit its bioavailability.

Human intestinal absorption (HIA) levels varied among the compounds, with most derivatives showing poor absorption (level 2). The 2WJO Ligand exhibited moderate absorption (level 1), while Donepezil and ZINC000614968635 showed good absorption (level 0), making them more favorable for oral bioavailability.

3.6. Metabolic stability and toxicity predictions.

The metabolic stability of the compounds was assessed based on CYP2D6 inhibition. None of the selected compounds was predicted to be CYP2D6 inhibitors, indicating a lower likelihood of drug-drug interactions involving this enzyme. Hepatotoxicity predictions indicated that all compounds, except ZINC000552367493 and the 2WJO Ligand, were non-hepatotoxic. The plasma protein binding (PPB) predictions indicated that all compounds exhibited high protein binding (PPB = TRUE), which may affect their in vivo distribution and clearance.

Table 6. Toxicity properties for benzimidazole derivatives and the reference drug.

Compound No	Mutagenicity	TD_{50} value (mg/kg)	LD_{50} value (g/kg)	EC_{50} value (mg/l)
		Carcinogenicity (Rat)	Acute oral toxicity (Rat)	Daphnia
ZINC000558477778	Non-Mutagen	4.60826	0.228686	0.737592
ZINC000558477776	Non-Mutagen	4.60826	0.228686	0.737592
ZINC000558477775	Non-Mutagen	4.60826	0.228686	0.737592
ZINC000558477777	Non-Mutagen	4.60826	0.228686	0.737592
ZINC000614968635	Non-Mutagen	9.04906	0.385389	8.10048
ZINC000552367493	Non-Mutagen	8.65317	0.317019	3.97125
Donepezil	Non-Mutagen	1.5591	0.389579	0.497697
2WJO Ligand	Non-Mutagen	92.9218	0.570354	0.02038

Table 6 summarizes the toxicity profiles of the benzimidazole derivatives. All compounds were predicted to be non-mutagenic, suggesting a favorable genotoxicity profile. The TD_{50} values, which indicate chronic toxicity potential, varied significantly, with donepezil displaying the lowest TD_{50} value (1.5591 mg/kg), suggesting higher chronic toxicity compared to the benzimidazole derivatives. Acute oral toxicity, represented by LD_{50} values, showed that the majority of benzimidazole derivatives had LD_{50} values ranging from 0.228686 to 0.385389 g/kg, suggesting moderate acute toxicity. The reference drug donepezil had a similar LD_{50} value (0.389579 g/kg), while the 2WJO Ligand exhibited the highest LD_{50} value (0.570354 g/kg), indicating lower acute toxicity. The EC_{50} values, representing the concentration required to produce a 50% maximal response in aquatic toxicity (Daphnia), varied among the compounds. The 2WJO Ligand exhibited the lowest EC_{50} value (0.02038 mg/L), indicating higher toxicity in aquatic environments, whereas other benzimidazole derivatives had relatively higher EC_{50} values, suggesting lower environmental toxicity.

The ADMET and toxicity analysis of benzimidazole derivatives indicates promising pharmacokinetic and safety profiles, with most compounds exhibiting favorable BBB permeability and non-mutagenic properties. However, solubility and intestinal absorption remain areas for improvement. The toxicity profile suggests that these derivatives are comparable to Donepezil in terms of acute and chronic toxicity, making them viable candidates for further optimization and in vivo evaluation.

4. Conclusions

The *in silico* screening of benzimidazole derivatives identified promising candidates for AChE and BACE-1 inhibition, two key therapeutic targets in Alzheimer's disease. The structure-based virtual screening workflow effectively refined a large compound dataset, selecting four high-affinity inhibitors using hierarchical docking (HTVS, SP, and XP). Among the identified compounds, ZINC000558477778 emerged as the top candidate for AChE inhibition, exhibiting the strongest binding affinity (-19.087 XP docking score) and significant interactions with key residues at both the CAS and PAS sites. Similarly, ZINC000614968635 was the most potent inhibitor of BACE-1, with an XP docking score of -7.43 and strong interactions with catalytic residues, suggesting its potential to reduce amyloid-beta production.

Notably, ZINC000558477776 and ZINC000558477775 displayed significant dual-target activity against both AChE and BACE-1, making them attractive candidates for multitarget-directed therapy. These compounds also exhibited favorable drug-likeness and ADMET profiles, supporting their potential as CNS-active agents. To confirm the stability and efficacy of these potential inhibitors, *in vitro* enzyme inhibition assays and in vivo studies are recommended. These additional studies will provide a deeper understanding of their binding stability, pharmacokinetic profile, and therapeutic potential, facilitating their advancement toward drug development for Alzheimer's disease.

Author Contributions

Conceptualization, Gigi G.P. and Uttam A. More; methodology, Gigi G.P.; software, Uttam A. More; validation, Gigi G.P., Uttam A. More, and Prema S.; formal analysis and investigation, Uttam A. More; resources, Gigi G.P., Prema S.; data curation, Uttam A. More; writing—original draft preparation, Uttam A. More; writing—review and editing, Gigi G.P., Uttam A. More, and Prema S.; visualization, Uttam A. More; supervision, Prema S. All authors have read and agreed to the published version of the manuscript.

Institutional Review Board Statement

Not applicable.

Informed Consent Statement

Not applicable.

Data Availability Statement

This research received no external funding

Funding

This research received no external funding.

Acknowledgments

The authors are grateful to the Department of Pharmaceutical Chemistry, Shree Dhanvantary Pharmacy College, Gujarat, India, for assistance with docking studies.

Conflicts of Interest

The authors declare no conflict of interest.

Supplementary materials

Download supplementary materials.

References

1. ALZHEIMER'S ASSOCIATION REPORT, 2021 Alzheimer's disease facts and figures. *Alzheimer's & Dementia* **2021**, *17*, 327-406, https://doi.org/10.1002/alz.12328.
2. De Strooper, B.; Karran, E. The Cellular Phase of Alzheimer's Disease. *Cell* **2016**, *164*, 603-615, https://doi.org/10.1016/j.cell.2015.12.056.
3. Hardy, J.; Selkoe, D.J. The Amyloid Hypothesis of Alzheimer's Disease: Progress and Problems on the Road to Therapeutics. *Science* **2002**, *297*, 353-356, https://doi.org/10.1126/science.1072994.
4. Vassar, R.; Kandalepas, P.C. The β-secretase enzyme BACE1 as a therapeutic target for Alzheimer's disease. *Alzheimer's Research & Therapy* **2011**, *3*, 20, https://doi.org/10.1186/alzrt82.
5. Gyimesi, M.; Okolicsanyi, R.K.; Haupt, L.M. Beyond amyloid and tau: rethinking Alzheimer's disease through less explored avenues. *Open biology* **2024**, *14*, 240035, https://doi.org/10.1098/rsob.240035.
6. Braak, H.; Braak, E. Neuropathological stageing of Alzheimer-related changes. *Acta Neuropathologica* **1991**, *82*, 239-259, https://doi.org/10.1007/BF00308809.
7. Iqbal, K.; Liu, F.; Gong, C.X.; Grundke-Iqbal, I. Tau in Alzheimer disease and related tauopathies. *Current Alzheimer research* **2010**, *7*, 656-664, https://doi.org/10.2174/156720510793611592.
8. Zheng, Q.; Wang, X. Alzheimer's disease: insights into pathology, molecular mechanisms, and therapy. *Protein & Cell* **2025**, *16*, 83-120, https://doi.org/10.1093/procel/pwae026.
9. Chen, Y.; Yu, Y. Tau and neuroinflammation in Alzheimer's disease: interplay mechanisms and clinical translation. *Journal of Neuroinflammation* **2023**, *20*, 165, https://doi.org/10.1186/s12974-023-02853-3.
10. Ghosh, A.K. BACE1 inhibitor drugs for the treatment of Alzheimer's disease: Lessons learned, challenges to overcome, and future prospects. *Global health & medicine* **2024**, *6*, 164-168, https://doi.org/10.35772/ghm.2024.01033.
11. Yan, R.; Vassar, R. Targeting the β secretase BACE1 for Alzheimer's disease therapy. *The Lancet. Neurology* **2014**, *13*, 319-329, https://doi.org/10.1016/s1474-4422(13)70276-x.
12. Coimbra, J.R.M.; Resende, R.; Custódio, J.B.A.; Salvador, J.A.R.; Santos, A.E. BACE1 Inhibitors for Alzheimer's Disease: Current Challenges and Future Perspectives. *Journal of Alzheimer's Disease* **2024**, *101*, S53-S78, https://doi.org/10.3233/JAD-240146.
13. Bazzari, F.H.; Bazzari, A.H. BACE1 Inhibitors for Alzheimer's Disease: The Past, Present and Any Future? *Molecules* **2022**, *27*, https://doi.org/10.3390/molecules27248823.
14. Egan Michael, F.; Kost, J.; Tariot Pierre, N.; Aisen Paul, S.; Cummings Jeffrey, L.; Vellas, B.; Sur, C.; Mukai, Y.; Voss, T.; Furtek, C.; Mahoney, E.; Harper Mozley, L.; Vandenberghe, R.; Mo, Y.; Michelson, D. Randomized Trial of Verubecestat for Mild-to-Moderate Alzheimer's Disease. *New England Journal of Medicine* **2018**, *378*, 1691-1703, https://doi.org/10.1056/NEJMoa1706441.
15. Watkins, E.A.; Vassar, R. BACE Inhibitor Clinical Trials for Alzheimer's Disease. J. Alzheimers Dis. 2024, 101 (s1), S41–S52. https://doi.org/10.3233/JAD-231258.
16. Sachin, V.K.; Sulagna, T.; Ning, W.; Valina, L.D.; Ted, M.D.; Xiaobo, M. Unraveling the tau puzzle: a review of mechanistic targets and therapeutic interventions to prevent tau pathology in Alzheimer's disease. *Ageing and Neurodegenerative Diseases* **2023**, *3*, 22, https://doi.org/10.20517/and.2023.20.
17. Birks, J. Cholinesterase inhibitors for Alzheimer's disease. *The Cochrane database of systematic reviews* **2006**, *2006*, Cd005593, https://doi.org/10.1002/14651858.Cd005593.
18. Whitehouse, P.J.; Price, D.L.; Struble, R.G.; Clark, A.W.; Coyle, J.T.; DeLong, M.R. Alzheimer's Disease and Senile Dementia: Loss of Neurons in the Basal Forebrain. *Science* **1982**, *215*, 1237-1239, https://doi.org/10.1126/science.7058341.
19. Suha, H.N.; Hossain, M.S.; Rahman, S.; Alodhayb, A.N.; Hossain, M.M.; Kawsar, S.M.A.; Poirier, R.A.; Uddin, K.M. *In silico* Discovery and Predictive Modeling of Novel Acetylcholinesterase (AChE)

Inhibitors for Alzheimer's Treatment. *Medicinal chemistry (Shariqah (United Arab Emirates))* **2025**, *21*, 345-366, http://doi.org/10.2174/0115734064304100240511112619.
20. Cavalli, A.; Bolognesi, M.L.; Minarini, A.; Rosini, M.; Tumiatti, V.; Recanatini, M.; Melchiorre, C. Multi-target-Directed Ligands To Combat Neurodegenerative Diseases. *Journal of Medicinal Chemistry* **2008**, *51*, 347-372, https://doi.org/10.1021/jm7009364.
21. Gong, C.-X.; Dai, C.-L.; Liu, F.; Iqbal, K. Multi-Targets: An Unconventional Drug Development Strategy for Alzheimer's Disease. **2022**, *Volume 14 - 2022*, https://doi.org/10.3389/fnagi.2022.837649.
22. Veerasamy, R.; Roy, A.; Karunakaran, R.; Rajak, H. Structure–Activity Relationship Analysis of Benzimidazoles as Emerging Anti-Inflammatory Agents: An Overview. *Pharmaceuticals* **2021**, *14*, https://doi.org/10.3390/ph14070663.
23. Chung, N.T.; Dung, V.C.; Duc, D.X. Recent achievements in the synthesis of benzimidazole derivatives. *RSC Advances* **2023**, *13*, 32734-32771, https://doi.org/10.1039/D3RA05960J.
24. Mohammed, L.A.; Farhan, M.A.; Dadoosh, S.A.; Alheety, M.A.; Majeed, A.H.; Mahmood, A.S.; Mahmoud, Z.H. A Review on Benzimidazole Heterocyclic Compounds: Synthesis and Their Medicinal Activity Applications. *SynOpen* **2023**, *07*, 652-673, https://doi.org/10.1055/a-2155-9125.
25. Bano, S.; Nadeem, H.; Zulfiqar, I.; Shahzadi, T.; Anwar, T.; Bukhari, A.; Masaud, S.M. Synthesis and anti-inflammatory activity of benzimidazole derivatives; an in vitro, in vivo and *in silico* approach. *Heliyon* **2024**, *10*, e30102, https://doi.org/10.1016/j.heliyon.2024.e30102.
26. Imran, M.; Al Kury, L.T.; Nadeem, H.; Shah, F.A.; Abbas, M.; Naz, S.; Khan, A.-u.; Li, S. Benzimidazole Containing Acetamide Derivatives Attenuate Neuroinflammation and Oxidative Stress in Ethanol-Induced Neurodegeneration. *Biomolecules* **2020**, *10*, https://doi.org/10.3390/biom10010108.
27. Karmaker, N.; Lira, D.N.; Das, B.K.; Kumar, U.; Rouf, A.S.S. Synthesis and Antioxidant Activity of Some Novel Benzimidazole Derivatives. *Dhaka University Journal of Pharmaceutical Sciences* **2018**, *16*, 245-249, https://doi.org/10.3329/dujps.v16i2.35263.
28. Başaran, R.; Kılcıgil, G.; Eke, B. Evaluation of the Antioxidant Activity of Some Imines Containing 1H-Benzimidazoles. *Turkish journal of pharmaceutical sciences* **2020**, *17*, 626-630, https://doi.org/10.4274/tjps.galenos.2019.05914.
29. Bhandari, S.V.; Nagras, O.G.; Kuthe, P.V.; Sarkate, A.P.; Waghamare, K.S.; Pansare, D.N.; Chaudhari, S.Y.; Mawale, S.N.; Belwate, M.C. Design, Synthesis, Molecular Docking and Antioxidant Evaluation of Benzimidazole-1,3,4 oxadiazole Derivatives. *Journal of Molecular Structure* **2023**, *1276*, 134747, https://doi.org/10.1016/j.molstruc.2022.134747.
30. Imran, M.; Shah, F.A.; Nadeem, H.; Zeb, A.; Faheem, M.; Naz, S.; Bukhari, A.; Ali, T.; Li, S. Synthesis and Biological Evaluation of Benzimidazole Derivatives as Potential Neuroprotective Agents in an Ethanol-Induced Rodent Model. *ACS chemical neuroscience* **2021**, *12*, 489-505, https://doi.org/10.1021/acschemneuro.0c00659.
31. Anastassova, N.; Aluani, D.; Kostadinov, A.; Rangelov, M.; Todorova, N.; Hristova-Avakumova, N.; Argirova, M.; Lumov, N.; Kondeva-Burdina, M.; Tzankova, V.; *et al*. Evaluation of the combined activity of benzimidazole arylhydrazones as new anti-Parkinsonian agents: monoamine oxidase-B inhibition, neuroprotection and oxidative stress modulation. *Neural regeneration research* **2021**, *16*, 2299-2309, https://doi.org/10.4103/1673-5374.309843.
32. Imran, M.; Al Kury, L.T.; Nadeem, H.; Shah, F.A.; Abbas, M.; Naz, S.; Khan, A.-u.; Li, S. Benzimidazole Containing Acetamide Derivatives Attenuate Neuroinflammation and Oxidative Stress in Ethanol-Induced Neurodegeneration. Biomolecules 2020, 10, 108. https://doi.org/10.3390/biom10010108.
33. Ferreira, L.G.; Dos Santos, R.N.; Oliva, G.; Andricopulo, A.D. Molecular Docking and Structure-Based Drug Design Strategies. *Molecules* **2015**, *20*, 13384-13421, https://doi.org/10.3390/molecules200713384.
34. Schrödinger, L. Schrödinger Release 2022-3: LigPrep. **2021**.
35. Alshamari, A.K.; Elsawalhy, M.; Alhajri, A.M.; Hassan, A.A.; Elharrif, M.G.; Sam, G.; Alamshany, Z.M.; Alshehri, Z.S.; Alshehri, F.F.; Hassan, N.A. Design, Synthesis, Molecular Docking and Biological Evaluation of Donepezil Analogues as Effective Anti-Alzheimer Agents. *Egyptian Journal of Chemistry* **2024**, *67*, 473-485, https://doi.org/10.21608/ejchem.2023.231046.8475.
36. More, U.; Patel, S.; Rahevar, V.; Noolvi, M.; Aminabhavi, T.; Joshi, S. *In silico* ADME and QSAR studies on a set of coumarin derivatives as acetylcholinesterase inhibitors against alzheimer's disease: CoMFA, CoMSIA, Topomer CoMFA and HQSAR. *Letters in Drug Design & Discovery* **2019**, *16*, https://doi.org/10.2174/1570180816666190712095907.

37. More, U.A.; Noolvi, M.N.; Kumar, D.; Tripathi, A. Exploring the Molecular Structural Requirements of Flavonoids as Beta- Secretase-1 Inhibitors Using Molecular Modeling Studies. *Current drug discovery technologies* **2023**, *20*, e290323215095, https://doi.org/10.2174/1570163820666230329090424.
38. Zhao, X.; Hu, Q.; Wang, X.; Li, C.; Chen, X.; Zhao, D.; Qiu, Y.; Xu, H.; Wang, J.; Ren, L.; Zhang, N.; Li, S.; Gong, P.; Hou, Y. Dual-target inhibitors based on acetylcholinesterase: Novel agents for Alzheimer's disease. *European journal of medicinal chemistry* **2024**, *279*, 116810, https://doi.org/10.1016/j.ejmech.2024.116810.
39. Ferreira, J.P.S.; Albuquerque, H.M.T.; Cardoso, S.M.; Silva, A.M.S.; Silva, V.L.M. Dual-target compounds for Alzheimer's disease: Natural and synthetic AChE and BACE-1 dual-inhibitors and their structure-activity relationship (SAR). *European journal of medicinal chemistry* **2021**, *221*, 113492, https://doi.org/10.1016/j.ejmech.2021.113492.
40. Irwin, J.J.; Sterling, T.; Mysinger, M.M.; Bolstad, E.S.; Coleman, R.G. ZINC: A Free Tool to Discover Chemistry for Biology. *Journal of Chemical Information and Modeling* **2012**, *52*, 1757-1768, https://doi.org/10.1021/ci3001277.
41. Schrödinger, L. LigPrep, Version 5.4, Schrödinger, LLC: 2021.
42. Hong, L.; Koelsch, G.; Lin, X.; Wu, S.; Terzyan, S.; Ghosh, A.K.; Zhang, X.C.; Tang, J. Structure of the Protease Domain of Memapsin 2 (β-Secretase) Complexed with Inhibitor. *Science* **2000**, *290*, 150-153, https://doi.org/10.1126/science.290.5489.150.
43. Schrödinger, L.L.C. Glide, Version 8.3, Schrödinger, LLC: New York, NY, 2021.
44. Friesner, R.A.; Banks, J.L.; Murphy, R.B.; Halgren, T.A.; Klicic, J.J.; Mainz, D.T.; Repasky, M.P.; Knoll, E.H.; Shelley, M.; Perry, J.K.; Shaw, D.E.; Francis, P.; Shenkin, P.S. Glide: a new approach for rapid, accurate docking and scoring. 1. Method and assessment of docking accuracy. *J Med Chem* **2004**, *47*, 1739-1749, https://doi.org/10.1021/jm0306430.
45. Schrödinger, L.L.C. *QikProp, version 2021*, Schrödinger, LLC: New York, NY, 2021.
46. Brooks, B.R.; Brooks Iii, C.L.; Mackerell Jr, A.D.; Nilsson, L.; Petrella, R.J.; Roux, B.; Won, Y.; Archontis, G.; Bartels, C.; Boresch, S.; Caflisch, A.; Caves, L.; Cui, Q.; Dinner, A.R.; Feig, M.; Fischer, S.; Gao, J.; Hodoscek, M.; Im, W.; Kuczera, K.; Lazaridis, T.; Ma, J.; Ovchinnikov, V.; Paci, E.; Pastor, R.W.; Post, C.B.; Pu, J.Z.; Schaefer, M.; Tidor, B.; Venable, R.M.; Woodcock, H.L.; Wu, X.; Yang, W.; York, D.M.; Karplus, M. CHARMM: The biomolecular simulation program. *Journal of Computational Chemistry* **2009**, *30*, 1545-1614, https://doi.org/10.1002/jcc.21287.

Publisher's Note & Disclaimer